Predicting Fractionator Dynamics by Using a Frequency Domain Solution Technique

R. E. BOLLINGER

Esso Mathematics and Systems, Inc., Florham Park, New Jersey

Methods are described for predicting the dynamic behavior of high purity fractionators. The paper shows how to model both the composition and hydraulic response in towers with many trays and in towers which are subject to a variety of disturbances. The technique involves the transformation of the linear dynamic equations to the frequency domain and the solution of the resulting complex algebraic equations for specific values of frequency. The paper includes a description of the model formulation, solution, and validation, and applications including the design of feedforward controllers.

Knowledge of the dynamic response of fractionation columns is a prerequisite to control system design, simulation, and trouble shooting. Costly plant testing has been the primary means of obtaining accurate dynamic data in the past. However, correlations of experimental data have proved increasingly unsatisfactory in towers achieving high purities and recoveries. As an alternative to plant testing, theoretical predictions of tower dynamics are often considered. However, the analysis of high purity towers presents serious numerical problems. Inability to control such towers can be particularly costly, since it is their purpose to recover valuable components. To insure that products will meet specifications, one often operates a poorly controlled fractionator at unnecessarily severe conditions in order to guarantee that average product quality will be satisfactory. High economic debits are associated with such operations.

Techniques are presented in this paper for overcoming the three primary difficulties encountered in predicting the dynamics of high purity fractionators. The first difficulty is the sheer size of the system, many towers have over one hundred trays. Second is the large number of disturbances which must be considered, for example, feed rate, composition, and enthalpy; heat loss through tower walls, cooling water temperature, reboiler duty. We would like to be able to predict the individual effect of each of these disturbances. Third is the vast difference in response rate between hydraulic effects (on the order of minutes) and composition effects (on the order of hours). Computing time limitations rule out the use of standard numerical integration techniques for considering these effects simultaneously.

This paper describes the use of a frequency domain solution technique for predicting the linearized dynamic behavior of large fractionators. The technique involves the transformation of the linear dynamic equations to the frequency domain and the solution of the resulting complex algebraic equations for specific values of frequency. In the first half of the paper, we present a discussion of the model, solution methods, and the results of studies made to validate the model. The second half of the paper covers applications of these techniques. Examples include the design of feedforward controllers and the side studies which have revealed the influence of nonlinearities, tray inefficiencies, and tray mixing on tower dynamics.

R. E. Bollinger is with Union Carbide Corporation, New York, New York.

NATURE OF MODEL DICTATED BY ANTICIPATED USE

Innumerable models can be conceived for representing fractionator dynamics. Many physical assumptions must be made in any case; these will be discussed shortly. However, the choice between a linear or a nonlinear model is at least as important as physical assumptions.

For some applications, a nonlinear model is essential. For example, to predict the response to a large (defined more precisely later) disturbance, such that column conditions will be taken far from their initial state, we need a nonlinear model. Large disturbances can generate nonlinear responses because physical properties and equilibrium data change with composition and because hydraulic behavior is irregular. Another example, where a nonlinear model is needed, is a multicomponent system, subject only to small disturbances but having a distributed component.

Fortunately, not all fractionator dynamics problems are so nonlinear as the two cited above. When the key components dominate and operation about a predetermined steady state is desired, linear and even two-component models often suffice. Furthermore, the advantages of linear models compel the engineer to consider their use. The most apparent advantage is that linear models can be efficiently solved. Just how efficiently will be demonstrated. Not only can they be solved for a single disturbance, but, for trivial additional effort, they can be solved for multiple disturbances and the individual effect of each disturbance can be determined. This, too, will be demonstrated.

With linear models, the answers are not only cheap from the standpoint of computing time but, in addition, they are in a form which can be easily simplified and represented as transfer functions for use in control system studies. By contrast, nonlinear computations must be repeated each time a different disturbance is considered, and the conversion of such results into transfer function form is less direct.

The aim of the work described in this paper was to predict the dynamics of large columns whose primary function was to split two components present in large concentration. Furthermore, fluctuations around a steady state were of principal interest. Because linear models are applicable to this problem and because of their attractive features, linear models have been employed in this work.

The specific model used was based on that proposed by

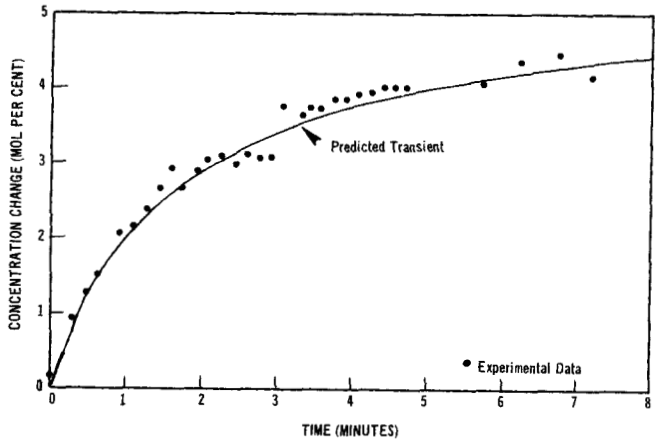

Fig. 1. Comparison of experimental and predicted transients, top tray in acetone-benzene separation.

Lamb, Pigford, and Rippin (7) in 1961. Reference is made to their paper for a detailed formulation of the equations. However, extensions to their model, and some of the physical assumptions, will be mentioned briefly.

The major addition to the basic model is the inclusion of an energy balance on each tray. This balance considers the effect of changing liquid holdup [holdup is assumed to vary with liquid flow rate as predicted by the Francis weir formula (*12*)] and includes a term representing heat exchange through walls of the column. Energy equations allow one to consider hydraulic effects which were not included in the original Lamb, Pigford, Rippin model. The model described in this paper also has the ability to consider multiple feed trays, drawoffs of either vapor or liquid side streams, tray efficiencies, and arbitrary models for the reboiler and condenser.

The model equations are obtained by writing component balances and heat balances for each tray together with the associated vapor-liquid equilibrium relationship, overall tray efficiencies, enthalpies as functions of temperatures, weir formulas, and bubble point relationships to yield a set of nonlinear differential equations. The following assumptions are made in the formulation of these equations:

1. Liquid on a tray is perfectly mixed so that the leaving liquid composition is equal to the average composition of the liquid holdup. Liquid held up in the downcomer is assumed to be inactive from the standpoint of mass transfer.

2. The gas phase is assumed to be perfectly mixed and at the same temperature as the liquid. (Violations of this temperature equality between the liquid and vapor on a given tray have been observed in columns separating components having widely differing boiling points. However, the assumption is sound in columns separating components of nearly equal boiling points.)

3. The pressure drop across each tray, overall tray efficiency, vapor volume above each tray, heat capacity, liquid density, and the equilibrium constants are assumed to be constant with time. (However, note that each of these variables can be different on different trays.)

These assumptions are based on physical knowledge of the fractionator and have been successfully used in other models (*1, 4, 6, 10, 13*). The assumption of constant pressure drop is based on data which indicate that pressure fluctuations are transmitted throughout the column in a matter of seconds. The transient effect of vapor flow rate on pressure drop is ignored.

The nonlinear equations which result from this formulation are given in Appendix A. Also given in that Appendix is the result of linearizing the nonlinear equations about a steady state. It is these linear equations whose solution we are seeking.

TRANSFORM METHOD EFFECTIVE

Let us next consider the specific technique used to solve the set of several hundred linear differential equations represented by Equation (1):

$$\mathbf{D}\frac{d\underline{x}}{d\theta} + \mathbf{F}\,\underline{x} = \underline{B}\,V \qquad (1)$$

$$\underline{x}(0) = 0$$

Transform methods are commonly applied to such problems. Classically, this consists of taking the Laplace transform

$$\mathbf{A}(s)\,\overline{\underline{x}}(s) = \underline{B}(s)\overline{V}(s) \qquad (2)$$

and solving for an $\overline{x}_i(s)$ of interest.

The result is an analytic transfer function which can be used in either of two ways. First, it can be analytically inverted to the time domain giving the time response $x_i(t)$ to an impulse disturbance in the independent variable represented by V. Second, the Laplace transform variable s can be replaced by $i\omega$, where ω is frequency, and the gain and phase angle of the transfer function plotted vs. log ω in the form of a Bode plot. For control studies, the second route is customarily followed.

An analytic solution, as described above, cannot be obtained on a system of equations as large as that in Equation (1). However, we can generate Bode plots, as in the second approach cited above, and thus achieve a result which is useful in control work (*11*). Instead of Laplace transforming, we take a Fourier transform which essentially means that s in Equation (2) is replaced by $i\omega$ as in Equation (3):

$$\mathbf{A}(i\omega)\overline{\underline{x}}(i\omega) = \underline{B}(i\omega)\overline{V}(i\omega) \qquad (3)$$

For any numerical value of ω, Equation (3) is a set of linear algebraic equations with constant complex coefficients. The solution for the selected value of ω, say $\omega = K$, is

$$\overline{\underline{x}}(iK) = \mathbf{A}(iK)^{-1}\,\underline{B}(iK)\overline{V}(iK) \qquad (4)$$

Comments on the inversion appear below. Note that the real and imaginary parts of the $\mathbf{A}^{-1}\,\underline{B}$ vector determine the gain [$G = (\text{real}^2 + \text{imag}^2)^{1/2}$] and phase angle ($\theta =$ arctan imag/real) for one frequency ($\omega = K$) of the transfer functions which we are to display on Bode plots. Since $\overline{\underline{x}}(iK)$ is a vector, there are points for m Bode plots, one for each of the dependent variables. Complete Bode plots can be generated by repeatedly solving Equation (3) for different values of ω.

The major computational effort in the above procedure is the inversion of $\mathbf{A}(i\omega)$. This step is not influenced by the nature of the independent variables (vector $\underline{B}\,V$). Thus, the inverse $\mathbf{A}(i\omega)^{-1}$ can be multiplied by several different $\underline{B}\,V$ vectors to generate points on Bode plots corresponding to a variety of disturbances. In summary, the inversion of $\mathbf{A}$ for one value of ω and the multiplication of that inverse by $n(\underline{B}\,V)$ vectors yields points on the Bode plots relating all m dependent variables to all of the n independent, or disturbance, variables.

Because the inversion of $A(i\omega)$ is so time-consuming, it deserves further attention. At the same time, it is convenient to illustrate the method used to handle several independent variables (or several $\underline{B}\,V$ vectors). For this purpose, we make $\underline{V}$ the vector of unit impulse disturb-

ances in the independent variables. $\underline{B}$ becomes a matrix having a row for each dependent variable and a column for each independent variable and contains the coefficient by which unit disturbances are multiplied in each equation. Rewriting Equation (3), we get

$$\mathbf{A}(i\omega)\underline{\bar{x}}(i\omega) = \mathbf{B}(i\omega)\underline{\bar{V}}(i\omega) \qquad (5)$$

Equation (5) could be solved by premultiplying both sides by the inverse of A:

$$\mathbf{A}^{-1}\mathbf{A}\underline{\bar{x}}(i\omega) = \mathbf{A}^{-1}\mathbf{B}\underline{V} \qquad (6)$$

The same result is obtained more conveniently by making a series of elementary row transformations to A and B until A is transformed to the identity matrix. As A is transformed to the identity matrix, B is transformed to the $\mathbf{A}^{-1}\mathbf{B}$ product. The i, j element of the matrix $\mathbf{A}^{-1}\mathbf{B}$ is the transfer function relating the j^{th} disturbance to the i^{th} dependent variable.

The second of the two methods described above is preferred because it allows many more equations to be treated. This advantage is realized whenever the equations and dependent variables can be arranged so that all elements of A are zero except those on the main diagonal and on several superdiagonals and subdiagonals. This is always possible with fractionators. A can then be transformed, by using a Gauss-Jordan reduction, so that no nonzero elements are generated outside its original group of diagonals. The number of storage locations which must be reserved for A is then equal to the number of elements in these diagonals. If $\mathbf{A}^{-1}$ were generated, a storage location would be required for each element in A.

So that A will have the form just described, all equations pertaining to a given tray are grouped and arranged in the order mass balance, component balance, heat balance, a bubble point equation, and an extra equation. The extra equation is used for adding controller relations. The variables for a given tray are arranged in the order liquid flow rate, liquid composition, vapor flow rate, temperature, and a control variable. When a control equation is not needed, a 1 is entered on the main diagonal and 0 in the remainder of the row and column.

In summary, the above procedure numerically generates Bode plots which relate responses of all dependent variables to disturbances in all independent variables. Its efficiency is demonstrated by the fact that a seventy-five-tray column was solved in less than 5 min. on an IBM-7094.

Before these results were used, they had to be validated experimentally. Several validation studies are described in the next section.

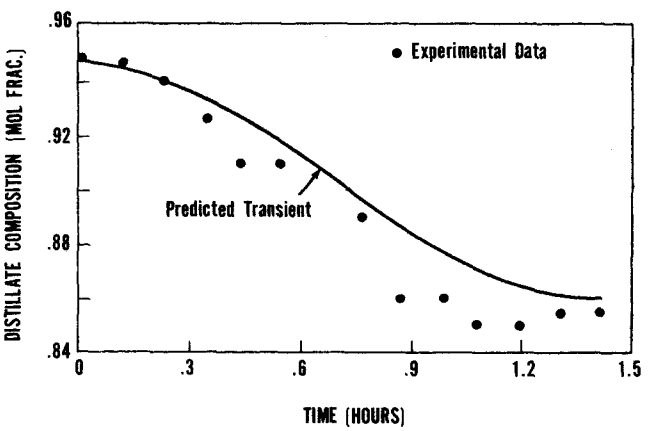

Fig. 2. Comparison of experimental and predicted transients, distillate composition from butane-isobutane fractionator.

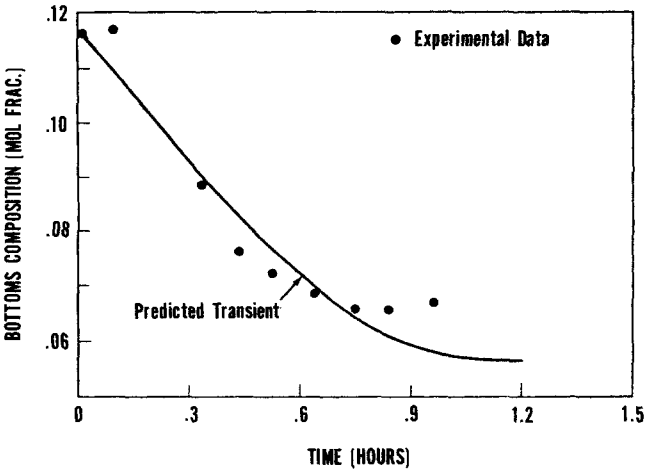

Fig. 3. Comparison of experimental and predicted transients, bottoms composition from butane-isobutane fractionator.

MODEL VERIFIED BY EXPERIMENTATION AND COMPUTATION

Both experimental and computational results were used to estimate the domain of accuracy of the linear model. The accuracy of the basic model had already been demonstrated by Baber (*1*). In Figure 1, his experimental data are compared with the results from the more detailed model described above. As expected, the agreement is excellent. The negligible difference between the basic and detailed models on Baber's system (acetone-benzene) shows that an assumption of equal molal overflow is valid for that system.

Comparison was also made with data from a seventy-five-tray butane-isobutane fractionator. Measurements were made of the composition response of the distillate and bottoms streams to a step change in feed flow rate. Results are shown in Figures 2 and 3. Predicted response is slightly slower than that observed experimentally. However, agreement is satisfactory in view of the accuracy of the experimental data.

Reference was also made to the computational results of Stanfield (*14*) which show the effect of nonlinearities on the dynamic response of large fractionators. This work indicates that open loop behavior is increasingly nonlinear as product purities increase. Columns producing an impure product either top or bottom will be more linear. Columns controlled around a steady state (say ±5 mole %) are also observed to be nearly linear. In addition, it was demonstrated that nonlinearities in the dynamic response are accompanied by nonlinear steady state changes. Thus, the degree of nonlinearity in the dynamic responses can be estimated by comparing the change in steady state predicted by linear and nonlinear steady state models. Nonlinear steady state models are widely available (*5*).

RESULTS VALUABLE FOR CONTROL SYSTEM DESIGN

Previous paragraphs describe a technique for computing points on Bode plots relating the response of dependent variables in a fractionator to variations in a number of different independent variables. This information is generated at frequencies of interest to the user. The results for $\omega = 0$ describe steady state changes. The value of these results is discussed before the complete dynamic results are mentioned. Both types of information are useful in control applications.

Results for $\omega = 0$, which are the steady state gains of the transfer functions, give the steady state changes expected in the dependent variables when unit step changes occur in the independent variables. These data reveal the

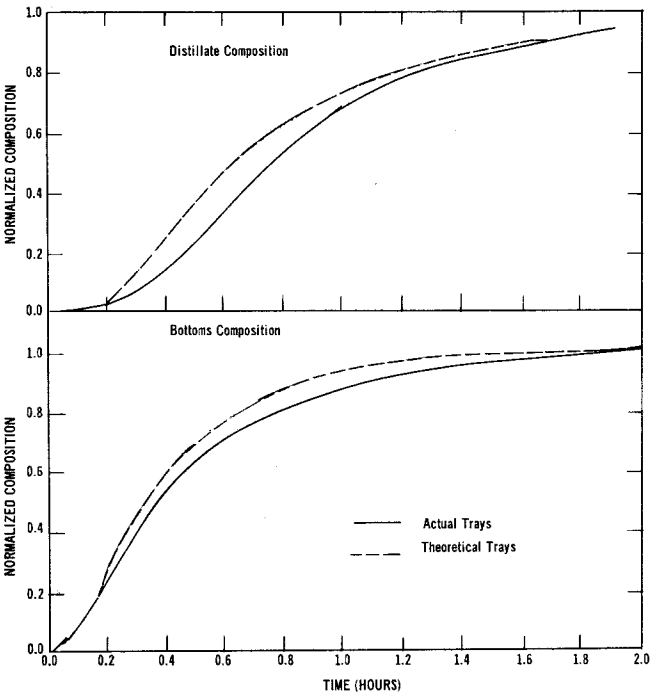

Fig. 4. Comparison of transients from a model having the actual number of trays and a model representing only the theoretical trays.

significance of disturbances in variables such as feed rate, composition and enthalpy, heat loss through tower walls, cooling water temperature and reboiler duty, and show how the steady state profiles of composition, temperature, liquid, and vapor flow rates will respond.

A use of the steady state results is in the design of steady state feedforward controllers. Such controllers are a special case of dynamic feedforward controllers, and these are discussed below.

In order to obtain dynamic information, we solve the model equations for values of ω other than zero. The user will choose a range of ω values depending on the phenomenon of interest. For example, high ω's must be selected to get information on hydraulics, whereas lower values contain information on composition dynamics. Ten values of ω are usually enough to provide a complete picture of the response. These Bode plots can be used in several ways:

1. Bode plots can be used as the basis for developing short-cut models of tower behavior.

2. The transfer function relating control tray temperature response to changes in reflux rate may be used as the basis for selecting constants in a three-mode controller. (The reflux rate could then be changed to a dependent variable, related to control tray temperature by the controller selected, and closed loop transfer functions could be computed.)

3. A minor rearrangement in the equations being solved can yield Bode plots which reveal what dynamic characteristics feedforward controllers should have. As an illustration, the following paragraphs describe the calculation of a feedforward controller to adjust reflux rates in response to feed rate variations so that distillate composition is constant.

The use of feedforward control for distillation columns has been described in several earlier papers (3, 8, 9). We describe, below, a method for calculating feedforward controllers using the approach described in this paper. To obtain the open loop response of the column, we solve a set of equations in which feed rate and reflux rate are independent variables, and distillate composition is a dependent variable. Denote the transfer functions giving the response of distillate composition to changes in feed rate and reflux by f_{xF} and f_{xR}, respectively. To eliminate composition variations, the reflux rate can be adjusted by a feedforward controller which receives a measurement of the feed flow rate. This feedforward controller should have the transfer function $-f_{xF}/f_{xR}$ (2).

Alternatively, this transfer function can be obtained directly by solving equations in which the distillate composition is an independent variable, and the reflux rate is dependent. [Referring to Equation (2), distillate composition is now in $\overline{V}(s)$, and the reflux rate is in $\overline{x}(s)$.] When the distillate composition is independent, we can hold it constant. The transfer function (now obtained directly) giving the response of reflux rate (now a dependent variable) to change in feed rate is the feedforward controller obtained above. It shows how reflux rate must be changed, as feed rate changes, if distillate composition is to remain constant.

When reflux rate is dependent, there are transfer functions giving its response to all disturbances (not just feed rate). These transfer functions are also feedforward controllers showing how reflux rate should be changed to eliminate the effect of the other disturbances on distillate composition. For a linear system, these signals can be added and reflux rates can be adjusted to eliminate the effect of variations in all measurable independent variables on distillate composition.

Similarly, feedforward controllers can be computed which hold several dependent variables constant in the face of disturbance. For example, feedforward controllers to eliminate deviations in both distillate and bottoms composition can be computed by making distillate and bottoms composition independent variables and by making reflux rate and reboiler duty dependent variables.

Having described several control applications, let us next mention studies made to determine the effect of downcomer holdup and tray efficiencies on fractionator dynamics. Downcomer holdup is easily added to the model formulation described earlier. In the previous formulation, the liquid composition leaving tray j and entering tray $j + 1$ were both called x_j. To represent downcomer holdup, we define the liquid composition entering tray $j + 1$ as $x_j^D(t) = x_j\ (t - T)$, where T is the dead time in the downcomer. In the frequency domain, dead time gives rise to an $e^{-i\omega T}$ factor ($e^{-i\omega T} = \cos \omega T - i \sin \omega T$). Dead time can be introduced by simply multiplying certain coefficients in the A matrix by the complex number $e^{-i\omega T}$.

Results indicated that inclusion of downcomer holdup had negligible effect on composition dynamics for reasonable values for T. Only when downcomer holdup was assumed to be several times the holdup on the tray did the response become noticeably slower.

Studies were also done to see if theoretical, rather than actual, trays could be used. Inefficient trays are easily represented in models of binary systems, but for multicomponent systems this is more difficult. It has been suggested that theoretical trays can be used if the holdup per tray is modified so that the total tray holdup in the entire column is the same as in the operating column. This proposal was tested on a seventy-seven-tray column having a tray efficiency of 65%. First a solution was obtained by using the actual number of trays and actual tray holdup. These results are represented by the solid lines in Figure 4. The dashed lines are computations on a column having fifty thoretical trays with holdup on each tray equal to the actual holdup divided by 0.65. It is seen in Figure 4 that the fifty-tray column, even with increased holdup per

tray, gives a faster response than the actual seventy-seven-tray column. This indicates that even for large columns it is necessary to deal with actual trays rather than simply maintaining constant total holdup in the column.

CONCLUSIONS

A technique has been described which is especially suited for predicting the dynamic response of large fractionators achieving sharp separations. The method is effective for fractionators having over one hundred trays and can handle time constants which differ by an order of magnitude. The individual effect of many disturbances is determined in a single solution.

The results are useful in doing control studies and for synthesizing feedforward controllers. Finally, computational experiments have shown the negligible effect of downcomer holdup and quantified the error introduced by using theoretical, instead of real, trays.

ACKNOWLEDGMENT

The author is grateful to Esso Mathematics and Systems, Inc., and Esso Research and Engineering Company for permission to publish these results and to colleagues Drs. C. S. Hwa, R. B. Stanfield, and F. W. Pasterczyk for their contributions to this work.

NOTATION

A_{tj} = area of tray available for holdup, sq.ft.
$\mathbf{A}$ = square coefficient matrix, $\mathbf{A}(s) = \mathbf{D}s + \mathbf{F}$
B_j = drawoff flow rate from j^{th} tray
$\underline{B}$ = vector of m coefficients determined by the nature of the disturbances
b_j = x_j for liquid drawoff; y_j for vapor drawoff
$\overline{C}_{pj}$ = heat capacity of the liquid on the j^{th} tray, B.t.u./(mole) (°R.)
$\overline{\overline{C}}_{pj}$ = heat capacity of the vapor above the j^{th} tray, B.t.u./(mole) (°R.)
$\mathbf{D}$ = $m \times m$ matrix containing the coefficients of the derivative terms
E_{oj} = overall efficiency defined by Equation (A5)
F_j = feed flow rate entering j^{th} tray moles/hr.
$\mathbf{F}$ = $m \times m$ matrix containing the coefficients of the dependent variables
f_j = mole fraction of the more volatile component in the feed entering the j^{th} tray
f = unspecified function used in Equation (A21)
G_j = vapor space above j^{th} tray, cu.ft.
H_j = enthalpy of the vapor on the j^{th} tray, B.t.u./mole
h_j = enthalpy of the liquid on the j^{th} tray, B.t.u./mole
h = weir height, ft.
K_j' = slope of the equilibrium line, $y_j^*(x_j)$
L_j = liquid flow rate from j^{th} tray, mole/hr.
l_j = liquid head above weir, ft.
N_j = unspecified functions used in Equation (A21)
P_j = pressure on the j^{th} tray, lb./sq.in.abs.
Q_j = heat loss through the walls of the j^{th} stage, B.t.u./hr.
R = universal gas constant, 10.73 (lb./sq.in.abs.)(cu.ft.)/(mole)(°F.)
S_j = liquid holdup on the j^{th} tray, mole
s = Laplace transform variable, $hr.^{-1}$
T_j = temperature of the liquid and vapor on the j^{th} tray, °R.
V_j = vapor flow rate from j^{th} tray, mole/hr.
V = disturbance, for example, feed rate, reboiler duty
w_j = perimeter of inside surface of downcomer, ft.
$\underline{x}$ = column vector of m dependent variables (flows, compositions, temperatures)
x_j = liquid mole fraction of the more volatile component on the j^{th} tray
y_j = vapor mole fraction of the more volatile component on the j^{th} tray
z_j = variables listed on the right side of Equation (21)

Greek Letters

θ = time, hr.
$\overline{\lambda}_j$ = heat of vaporization on the j^{th} tray, B.t.u./mole
ρ_j = vapor density above j^{th} tray, mole/cu.ft.
ρ_{Lj} = liquid density on j^{th} tray, mole/ cu. ft.
τ = total number of variables
τ^* = number of variables normalized
ϕ_j = enthalpy of the feed entering the j^{th} tray, B.t.u./mole
Ψ_j = h_j for liquid drawoff; H_j for vapor drawoff
ω = frequency, $hr.^{-1}$

Superscripts

$'$ = perturbation from steady state
$''$ = normalized perturbation
$—$ = steady state value
$*$ = value at equilibrium

Subscripts

0 = distillate
1 = reflux
2 = top tray
N = reboiler
$N-1$ = last tray

LITERATURE CITED

1. Baber, M. F., and J. A. Gerster, *AIChE J.*, 8, No. 3, 407 (July, 1962).
2. Bollinger, R. E., and D. E. Lamb, *Ind. Eng. Chem. Fundamentals*, 1, 245 (1962).
3. Cadman, T. W., and N. L. Carr, *ISA Trans.*, 5, 386 (1966).
4. Distefano, G. P., F. P. May, and C. E. Huckaba, *AIChE J.*, 13, 125 (1967).
5. Holland, C. D., "Multicomponent Distillation," Prentice Hall, Englewood Cliffs, N. J. (1963).
6. Huckaba, C. E., F. R. Franke, and F. P. May, paper presented at 55th Annual Meeting, Am. Inst. Chem. Engrs., Chicago, Ill. (1962).
7. D. E. Lamb, R. L. Pigford, and D. W. T. Rippin, *Chem. Eng. Progr. Symposium Ser. No. 56*, 60, 132 (1964).
8. Luyben, W. L., and J. A. Gerster, *Ind. Eng. Chem. Chem. Process Design Develop.*, 3, No. 4, 374 (1964).
9. MacMullen, E. C., and F. G. Shinskey, *Control Eng.*, 11, No. 3, 69 (1964).
10. Peiser, A. M., and S. S. Grover, *Chem. Eng. Progr.*, 58, 65 (Sept., 1962).
11. Rippin, D. W. T., and E. D. Lamb, *Chem. Eng. Progr. Symposium Ser. No. 36*, 57 (1961).
12. Robinson, C. S., and E. R. Gilliland, "Elements of Fractional Distillation," p. 410, McGraw-Hill, New York (1950).
13. Rosenbrock, H. H., A. B. Tavendale, C. Storey, and J. A. Challis, "Transient Behavior of Multicomponent Distillation Columns," Proc. IFAC Congr., Moscow (1960).
14. Stanfield, R. B., unpublished results.

Manuscript received May 20, 1968; revision received January 8, 1969; paper accepted January 31, 1969. Paper presented at AIChE St. Louis meeting.

APPENDIX A

The general balance equations and equilibrium relationships are presented below. These are followed by the linearized equations which are to be solved numerically.

Main Column Equations

The total material balance on the j^{th} tray is

$$\frac{d(S_j + \rho_j G_j)}{d\theta} = L_{j-1} + V_{j+1} + F_j - L_j - V_j - B_j \quad \text{(A1)}$$

S_j will be eliminated by using a weir formula. G_j will be assumed constant. ρ_j will eliminated by using a P, ρ, T relationship.

The component balance for the more volatile component on the j^{th} tray is

$$\frac{d(S_j x_j + \rho_j G_j y_j)}{d\theta} = L_{j-1}x_{j-1} + V_{j+1}y_{j+1} + F_j f_j - L_j x_j - V_j y_j - B_j b_j \quad \text{(A2)}$$

y_j will be eliminated by using a vapor-liquid equilibrium relationship and tray efficiency.

The energy balance on the j^{th} tray is

$$\frac{d(S_j h_j + \rho_j G_j H_j)}{d\theta} = L_{j-1}h_{j-1} + V_{j+1}H_{j+1} + F_j\phi_j - L_j h_j - V_j H_j - B_j \Psi_j - Q_j \quad \text{(A3)}$$

h_j and H_j will be expressed as functions of temperature.

The vapor-liquid equilibrium relationship on the j^{th} tray is

$$y_j^* = y_j^*(x_j) \quad \text{(A4)}$$

The overall efficiency for the j^{th} tray is defined as

$$E_{oj} = \frac{y_j - \bar{y}_j}{y_j^* - \bar{y}_j^*} \quad \text{(A5)}$$

The enthalpy-temperature relationship for the j^{th} tray is

$$h_j = \bar{C}_{Pj} T_j \quad \text{(A6)}$$

$$H_j = C_{Pj} T_j + \bar{\lambda}_j \quad \text{(A7)}$$

The Francis weir formula relates holdup and liquid flow rate:

$$S_j = \rho_{Lj} A_{tj}(h + l_j) \quad \text{(A8)}$$

$$l_j = 0.001915 \left(\frac{L_j}{\rho_{Lj} w_j}\right)^{2/3} \quad \text{(A9)}$$

The ideal gas law is used to express vapor density in terms of pressure and temperature:

$$\rho_j = \frac{P_j}{RT_j} \quad \text{(A10)}$$

A bubble point relationship gives temperature in terms of pressure and composition:

$$T_j = T_j(x_j, P_j) \quad \text{(A11)}$$

Equations (A1) to (A11) define, respectively, the variables L_j, x_j, V_j, y_j^*, y_j, h_j, H_j, S_j, l_j, ρ_j, T_j. Substitutions can be made to eliminate all the above variables, except L_j, x_j, V_j, and T_j, and yield one algebraic and three differential equations. A similar group of four equations must be written for each tray. The column, exclusive of the condenser and reboiler, is then defined if the following quantities are specified: G_j, F_j, B_j, f_j, ϕ_j, Q_j, K_j', E_{oj}, $\bar{C}_{Pj}$, $\bar{\bar{C}}_{Pj}$, $\bar{\lambda}_j$, ρ_{Lj}, A_{tj}, h, w_j, P_j. K_j' is the slope of the equilibrium line $y_j^*(x_j)$.

Condenser and Reboiler Equations

Equations must also be written for the condenser and reboiler. These equations will vary for each column, but their form can be given.

Condenser equations

Total material balance:

$$L_1 = L_1(L_0, V_2) \quad \text{(A12)}$$

or

$$L_0 = L_0(L_1, V_2) \quad \text{(A13)}$$

Component balance:

$$x_1 = x_1(x_2, T_1, T_2, P_1, L_1, L_0, V_2) \quad \text{(A14)}$$

Energy balance:

$$P_1 = P_1(x_1, T_1, T_2, L_1, L_0, V_2, T_c) \quad \text{(A15)}$$

Since the vapor flow rate from the condenser is zero, the energy balance can be used to determine P_1.

Bubble point relationship:

$$T_1 = T_1(P_1, x_1) \quad \text{(A16)}$$

Reboiler equations

Total material balance:

$$L_N = L_N(L_{N-1}, V_N) \quad \text{(A17)}$$

Component balance:

$$x_N = x_N(T_N, T_{N-1}, P_N, L_N, L_{N-1}, V_N, x_{N-1}) \quad \text{(A18)}$$

Energy balance:

$$V_N = V_N(T_{N-1}, T_N, L_{N-1}, L_N, V_S) \quad \text{(A19)}$$

Bubble point relationship:

$$T_N = T_N(P_N, x_N) \quad \text{(A20)}$$

Linearization of Dynamic Equations

The above formulation yields four equations for each tray, the condenser, and the reboiler. The dependent variables are the liquid flow rates and compositions, the vapor flow rates, and temperatures. The equations are of the form

$$N_1\frac{dL_j}{d\theta} + N_2\frac{dx_j}{d\theta} + N_3\frac{dP_j}{d\theta} + N_4\frac{dT_j}{d\theta} = f(L_j, L_{j-1}, x_{j+1}, x_j, x_{j-1}, V_j, V_{j+1}, T_{j+1}, T_j, T_{j-1}; G_j, F_j, B_j, f_j, \phi_j, Q_j, K_j', E_{oj}, \bar{C}_{Pj}, \bar{\bar{C}}_{Pj}, \bar{\lambda}_j, \rho_{Lj}, A_j, h, W_j, P_j) \quad \text{(A21)}$$

The first ten variables on the right-hand side are dependent; the remaining factors are independent variables or constants.

To expedite computation and to permit the results to be generalized, the nonlinear equations are linearized. The linearization is about an initial steady state, and the results will be valid if the column operates near this steady state. Linearization is accomplished as follows:

1. Evaluate N_1, N_2, N_3, and N_4 at steady state.
2. Expand f in a Taylors series about the steady state.
3. Retain only the linear terms in the Taylors series.
4. Subtract the steady state equation which is obtained by setting all the derivatives in Equation (A21) equal to zero.

Equation (A21) becomes

$$\bar{N}_1\frac{dL_j'}{d\theta} + \bar{N}_2\frac{dx_j'}{d\theta} + \bar{N}_3\frac{dP_j'}{d\theta} + \bar{N}_4\frac{dT_j'}{d\theta} = \sum_{i=1}^{\tau}\left(\frac{\overline{\partial f}}{\partial z_1}\right) z_i \quad \text{(A22)}$$

It is convenient to normalize the flow rates, temperatures, and pressures with respect to their steady state values.

Equation (A22) then becomes

$$\bar{N}_1\bar{L}_j\frac{dL_j''}{d\theta} + \bar{N}_2\frac{dx_j'}{d\theta} + \bar{N}_3\bar{P}_j\frac{dP_j''}{d\theta} + \bar{N}_4\bar{T}_j\frac{dT_j''}{d\theta} = \sum_{i=1}^{\tau^*}\frac{\overline{\partial f}}{\partial z_1}\bar{z}_i z_i'' + \sum_{i=\tau^*+1}^{\tau}\frac{\overline{\partial f}}{\partial z_i} z_i' \quad \text{(A23)}$$

The only independent variables in the main column which are considered to vary with time are F_j, B_j, f_j, ϕ_j, Q_j, and P_j. Depending on the specific column configuration, additional independent variables appear in the condenser and reboiler equations. Since it is assumed that the pressure drop is not a function of time, the pressure perturbation on each tray is the same; that is, $P_j = P_1'$. The P_j'''s are not equal since the steady state pressures are, of course, different.